GENERALIZED THREE-BODY PROBLEM AND THE INSTABILITY OF THE CORE-HALO OBJECTS IN BINARY SYSTEMS

Andrzej Odrzywołek

The Marian Smoluchowski Institute of Physics, Jagiellonian University
Łojasiewicza 11, 30-348 Kraków, Poland

(Received March 18, 2015; revised version received June 16, 2015; final version received September 10, 2015)

The goal of this work is to construct a simplified model of the core-halo structures in binary systems, such as Thorne–Żytkov objects, hot Jupiters, protoplanets with large moons, red supergiants in binaries and globular clusters with central black hole. A generalized planar circular restricted three-body problem is investigated with one of the point masses, M, replaced with a spherical body of finite size. The mechanical system under consideration includes two large masses m and M, and a test body with small mass μ. Mass μ, initially, is placed at the geometric center of mass M, and shares its orbital motion. Only gravitational interactions are considered and the extended mass M is assumed to be rigid with rotational degrees of freedom neglected. Equations of motion are presented, and linear instability criteria are derived using quantifier elimination. The motion of the test mass μ is shown to be unstable due to the resonance between orbital and internal frequencies. In the framework of model, the central mass μ can be ejected if resonance conditions are met during the evolution of the system. The above result is important for core-collapse supernova theory, with mass μ identified with the helium core of the exploding massive star. The instability cause off-center supernova "ignition" relative to the center of mass of the hydrogen envelope. The instability is also inevitable during the protoplanet growth, with hypothetical ejection of the rocky core from gas giants and formation of the "puffy planets" due to resonance with orbital frequency. Hypothetical central intermediate black holes of the globular clusters are also in unstable position with respect to perturbations caused by the Galaxy. As an amusing example, we note that the Earth–Moon or the Earth–Sun systems are stable in the above sense, with the test body μ being a hypothetical black hole created in the high-energy physics experiment.

DOI:10.5506/APhysPolB.46.2555
PACS numbers: 98.20.Gm, 97.82.–j, 95.10.Fh

1. Introduction

Traditional classical mechanics approaches to astrophysical binaries usually assume that mechanical system can be described in terms of point masses. However, in many important situations, this assumption is not valid, *e.g.*, the motion of a spacecraft in the gravitational field of a non-spherical asteroid [1] requires a more general description [2]. In astrophysics, we frequently deal with core-halo objects which possess spherical symmetry, however their total mass is unevenly divided into nearly point-like central object and extensive low-density envelope. For example, all red-giants are composed of small, high-density helium core of mass ~ 4–$5\ M_\odot$, surrounded by a low-density envelope whose mass varies by orders of magnitude from few solar masses up to $\sim 100\ M_\odot$ [3].

Gaseous giant planets ("Jupiters") are composed of a rocky core and an extended envelope. Inside icy moons (*e.g.* Europa, Enceladus) and exoplanets ("blue ocean" super-earths, see [4]), we also find a rocky core, this time "floating" in the surrounding liquid ocean [5, 6]. Therefore, in some situations, aforementioned bodies should be treated as two-component structures.

Globular cluster (GC) with central intermediate-mass black hole (IMBH, see [7–13]) is another very important case of the core-halo object. Since non-gravitational effects are essentially negligible in GC–IMBH system, it provides a perfect testbed for our model.

There are also more exotic examples: the Thorne–Żytkow object [14] composed of a central neutron star or black hole and a normal star [15–17], non-standard Solar model with black hole inside [18, 19], or a tiny black hole created on Earth in a high-energy experiment [20–22].

We are interested in the situation where the core-halo system is a part of an orbiting gravitationally bound system. For red giants, it would be a binary companion star. For planets: moons, and *vice versa*. For globular clusters, it is the host Galaxy. In all above examples, binary interaction effects, *e.g.*, tidal interactions, are known to be non-negligible. In extreme cases, mass transfer or a total disruption of one component is possible. Are there other types of instability, resonant in particular? We try to answer this question in the framework of mechanical model.

An original motivation for the model to be described below is the suggestion of [23] that in the core-collapse supernovae, the iron core might be displaced with respect to the geometric symmetry center of the extended and usually much more massive hydrogen envelope. Arnett and Meakin [23] proposed hydrodynamical $L = 1$ instabilities during Si burning as a main cause of the displacement. They wrote: *If there were a driving mechanism for core-mantle oscillation, here would be an asymmetry due to the displacement of the core and mantle relative to the center of mass.* Here, we propose another mechanism: gravitational instability in the binary core-halo system.

The point mass in the center of an extended object starts oscillating when it is perturbed (displaced) from the central position. Is this position stable with respect to perturbations caused by the third body orbiting outside? If we could tune internal and orbital frequencies simultaneously providing unlimited supply of energy in the form of driving force, the answer is yes. However, we are dealing with an energy-conserving system. Many years of struggle to answer very similar questions in the classic three-body problem [24] suggest caution, and rigorous mathematical approach.

The article is organized as follows. In Sect. 2, we present details of the model describing core-halo system in binary. The standard framework based on restricted planar circular three-body problem is presented in Subsect. 2.1, together with linear stability analysis for the uniform density ball. In Subsect. 2.2, we solve numerically the full system and confirm the linear instability criterion in the non-linear regime. In Subsect. 2.3, much more general model with non-planar motion and a third body of finite mass μ is provided. Potential astrophysical applications of the instability are discussed in Sect. 3: massive pre-supernova stars (Subsect. 3.1), (exo)planets and moons (Subsect. 3.2) and globular clusters with IMBH (Subsect. 3.3). Finally, the importance of the proposed mechanism of instability, limitations of mechanical model, and the chances for observational verification and directions of future research are summarized in concluding Sect. 4.

2. Derivation and numerical verification of the instability criteria

2.1. Restricted planar circular three-body problem approach

To handle dynamics of a core-halo object in a binary system, we propose the following model. Mechanical system of interest (*cf.* Fig. 1) includes two masses m and M orbiting the center of mass on circular orbits. The mass m (first body) is a point mass. The mass M (second body) is an extended spherical rigid body with known density $\rho(r)$. Rotational degrees of freedom for mass M are neglected. Third body is a test body, so its mass is assumed to be negligible (see Subsect. 2.3 for more general model with this assumption relaxed). In this subsection only, in order to simplify formulae, and facilitate derivation of linear instability criteria, we further assume that density $\rho(r)$ inside mass M is constant. Additionally, mass m is assumed to orbit outside radius R of mass M. This allows us to use classic restricted planar circular three-body problem formulae. The distance between the center of mass M and m is equal to d, and $d \geq R$. The third test body is initially in the center of mass M, where also coordinate origin is placed. In the co-rotating Cartesian system (x, y) (*cf.* Fig. 1), equations of motion for the third body, restricted to orbital plane, are

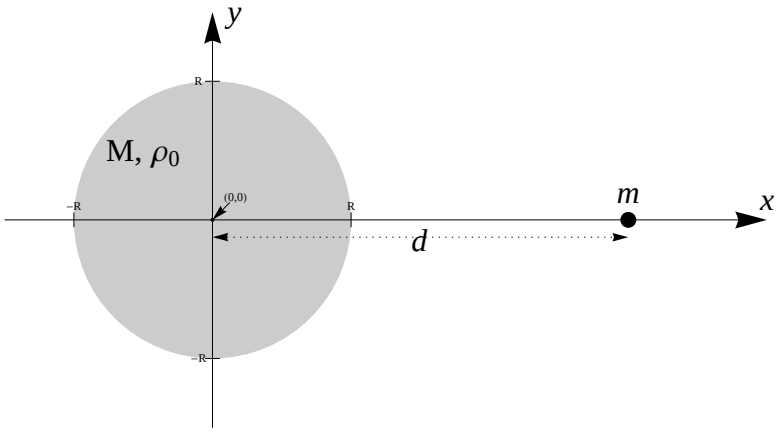

Fig. 1. Co-rotating coordinate system used to derive (1).

$$\ddot{x} - 2\,\omega\,\dot{y} + k\,x + \frac{G\,m\,(x-d)}{[(x-d)^2+y^2]^{3/2}} + \frac{G\,m}{d^2} = 0\,, \tag{1a}$$

$$\ddot{y} + 2\,\omega\,\dot{x} + k\,y + \frac{G\,m\,y}{[(x-d)^2+y^2]^{3/2}} = 0\,, \tag{1b}$$

where the dot denotes the time derivative. The frequency ω is given by Kepler's third law

$$\omega^2 = \frac{G\,(m+M)}{d^3} \tag{2}$$

and

$$k = \tfrac{4}{3}\pi G\rho - \omega^2\,. \tag{3}$$

System (1) is very similar to the classical planar restricted circular three-body problem, see [25]. Without terms *explicite* involving gravitational constant G, system (1) describes the Foucault pendulum [26].

The conserved energy for system (1) is

$$E = \frac{1}{2}\dot{x}^2 + \frac{1}{2}\dot{y}^2 + U(x,y)\,, \tag{4a}$$

$$U(x,y) = \frac{1}{2}k\,\left(x^2+y^2\right) - \frac{G\,m}{\sqrt{(x-d)^2+y^2}} + \frac{G\,m(x+d)}{d^2}\,. \tag{4b}$$

Equations of motion (1) and energy (4b) with constant k are suitable for analysis of the small (linear) perturbations of the test body only. To explore non-linear effects, in particular possible ejection of the test body from mass M, we have to use the model with non-constant density $\rho(r)$. This is done in Sect. 2.2.

Linearization of equations (1) for small perturbations around point $x = 0$, $y = 0$ is done as follows. After substitution $x(t) = \epsilon\,\zeta(t), y(t) = \epsilon\,\xi(t)$ into (1), series expansion has been calculated with respect to ϵ, and higher-order terms dropped. Following linear system, it has been obtained

$$\ddot{\zeta} - 2\,\omega\,\dot{\xi} + (k - 2q)\,\zeta \;=\; 0\,, \tag{5a}$$

$$\ddot{\xi} + 2\,\omega\,\dot{\zeta} + (k + q)\,\xi \;=\; 0\,, \tag{5b}$$

where

$$q = \frac{G\,m}{d^3}\,. \tag{6}$$

Eigenvalues λ of system (5) are solutions to the algebraic equation

$$\left(\lambda^2 + k - 2q\right)\left(\lambda^2 + k + q\right) + 4\,\omega^2 = 0\,. \tag{7}$$

The system is considered linearly unstable with respect to small perturbations if at least one solution of (7) has a positive real part $\mathrm{Re}(\lambda) > 0$.

Resolving above conditions leads us to the instability criteria

$$\frac{M}{d^3} < \frac{4}{3}\pi\rho \;<\; \frac{M + 3\,m}{d^3}\,, \tag{8a}$$

$$\frac{4}{3}\pi\rho \;<\; \frac{1}{2}\frac{m}{d^3}\frac{M - m/8}{M + m}\,. \tag{8b}$$

Criteria (8) has been verified solving (1) numerically, and solving linearized system (5) analytically. Result (8a) can be obtained from analysis of potential (4b) extremum at $x = 0, y = 0$ as well. The left-hand side of (8a), *i.e.*, condition $M/d^3 < 4/3\pi\rho$, is trivial from astrophysical point of view, because the central density cannot be smaller than average density. In any realistic astronomical body, density decrease outwards: $\rho(r) \le \rho(0)$. The same argument apply to (8b). Even in the most favorable situation $m = 2M$, the central density should be less than half of the average density for mass m for this instability to occur[1].

If we assume that density decreases outwards from the center, we may simply write simplified form of (8), relevant to the astrophysical applications

$$\frac{4}{3}\pi\rho < \frac{M + 3\,m}{d^3}\,. \tag{9}$$

It is instructive to compare this instability criterion with the Roche stability limit [27, 28]

$$\frac{d}{R} > \kappa\left(\frac{m}{M}\right)^{1/3}\,, \tag{10}$$

where $\kappa = \sqrt[3]{3}$.

[1] However, an artificial body with such properties could be created, and experiments performed in micro-gravity at orbital station.

Re-writing (9) in terms of R instead of ρ and combining with (10), we obtain

$$\kappa \left(\frac{m}{M}\right)^{1/3} < \frac{d}{R} < \left(1 + \frac{3m}{M}\right)^{1/3} . \tag{11}$$

2.2. Numerical verification of the instability and the long-term behavior in non-linear regime

In the unstable case, the point mass is likely to abandon the central region. Then the entire density distribution $\rho(r)$, not just $\rho(0)$, becomes important. Location of "surface radius" defined as $\rho(R) = 0$ determines cases of "core ejection". The non-constant density changes linear harmonic oscillator force into the non-linear one. Introducing the mass function $m(r)$

$$m(r) = 4\pi \int_0^r \rho(\zeta)\zeta^2 d\zeta \,,$$

the system of equations of motion becomes similar to (1), but now

$$k = \frac{G\, m(r)}{r^3} - \omega^2 \,, \qquad r^2 = x^2 + y^2 \,. \tag{12}$$

System (1) with non-constant $k(x, y)$ given by (12) is more general, and covers astrophysically interesting cases with non-constant density.

Mass M is now given by

$$M \equiv m(R) = 4\pi \int_0^R \rho(\zeta)\zeta^2 d\zeta \,.$$

Let us note, if we allowed the mass m to orbit inside the region where $\rho(r) > 0$, then the inertial mass M_{inert} would be different from the gravitational mass M_{grav}. In such a situation, the circular two-body problem has a slightly different solution compared to the classic one. In particular, the Kepler frequency is given by

$$\omega^2 = G \frac{M_{\text{grav}} + m\frac{M_{\text{grav}}}{M_{\text{inert}}}}{d^3} \,. \tag{13}$$

In what follows, we assume that $R < d$, *i.e.*, the mass m orbits outside the mass M.

For general $\rho(r)$, we have the conserved energy

$$E = \frac{1}{2}\dot{x}^2 + \frac{1}{2}\dot{y}^2 + U(x,y)\,, \tag{14a}$$

$$U = \phi(r) - \frac{1}{2}\omega^2 r^2 - \frac{G\,m}{\sqrt{(x-d)^2+y^2}} + \frac{G\,m(x+d)}{d^2}\,, \tag{14b}$$

where $r = \sqrt{x^2+y^2}$ and the gravitational potential of the star is

$$\phi(r) = G\int_0^r \frac{m(\zeta)}{\zeta^2}\,d\zeta\,. \tag{15}$$

The simplest example, a uniform density ball of radius R, leads to a piecewise-constant density

$$\rho(r) = \begin{cases} \rho_0 & \text{for} \quad r < R\,, \\ 0 & \text{for} \quad r > R\,, \end{cases} \tag{16}$$

which by (15) gives the gravitational potential

$$\phi(r) = \begin{cases} \frac{2}{3}\pi G\rho_0 r^2 & \text{for} \quad r < R\,, \\ -\frac{GM}{r} + \frac{3}{2}\frac{GM}{R} & \text{for} \quad r > R\,. \end{cases} \tag{17}$$

Before presenting the numerical computations, it is helpful to understand possible trajectories qualitatively. Using energy considerations, we can find allowed regions on x–y plane. The test body at rest in the central point $x = 0$, $y = 0$ has the energy $E = 0$. Three typical cases are presented for uniform sphere of density ρ and radius R (dashed circle in Fig. 2). Energy had been perturbed with small positive value δE. Allowed Hill region $U(x,y) < \delta E$ has been shaded. In the stable situation, see Fig. 2 (a), we have three disconnected regions: the central region of mass M, the neighborhood of mass m, and the "outer space" extending to the infinity. The perturbed test body simply oscillates with frequency related to the central density, simultaneously rotating like the Foucault pendulum. In the presence of the drag, it will settle down at the geometrical center of mass M. When the density drops below the critical value, given by Eq. (9), the central region of mass M and region surrounding mass m become connected, *cf.* Fig. 2 (b). The test body begins to oscillate with growing amplitude forced by the gravitational pull of mass m. After some time, depending on the amplitude of initial perturbation, the test body is ejected from mass M and enters a chaotic orbit around mass m, see Fig. 2 (b), but it is still bounded with binary system. For the density much smaller than critical, all three

allowed regions become connected, and the test body will be ejected from the system, spiraling out to infinity (Fig. 2 (c)). The behavior described above has been confirmed by the numerical solution of system (1) with non-constant k from Eq. (12). Sample trajectories for uniform density ball are shown in Fig. 2.

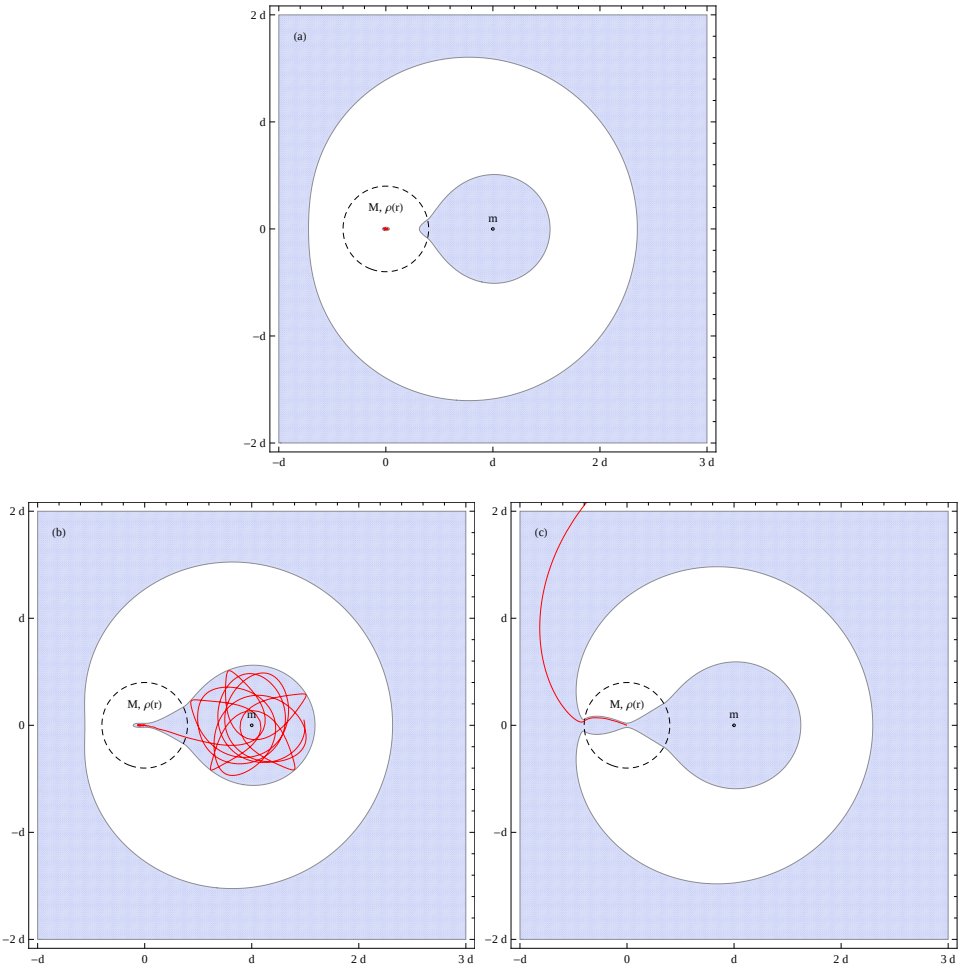

Fig. 2. Three typical cases of the dynamics: stable (a), unstable chaotic (b), unstable with ejection (c). Shading has been used to show regions allowed to motion by energy conservation. Potential barrier (white) prevents escape to infinity for linearly unstable case (b).

Instability is not a resonance with Kepler frequency (2), because instability criterion (8a) involves additional factor 3 before mass m. However, using the language of resonances, we can easily understand the underlying physics [24]. Consider the classical first-year student textbook example of uniform density ball with radius R and satellite in circular orbit just above the surface ($d = R$). Then, the internal harmonic oscillator and orbital frequencies are identical. Therefore, the test mass in the center is in resonance with the small mass in orbit. However, astrophysical bodies are centrally condensed ($\rho_c > \bar{\rho}$) and binary companions are usually more distant ($d > R$), so this resonance disappears. But the orbital frequency depends on both masses M and m. By increasing the mass m, we can make these frequencies equal again. Note that we have never assumed that the mass M is dominant, so the mass m may be arbitrarily large.

An inevitable presence of the dynamic drag inside gaseous objects (including GC, see [29]) and other forms of friction forces acting on a test body inside mass M has, surprisingly, only a minor effect on resulting dynamics, at least in the framework of our model. The drag suppresses the amplitude of oscillations and delays the onset of instability. However, in the resonant regime, point $x = 0, y = 0$ has a "top-hill" position in the potential landscape given by equation (14b). In effect, the global dynamics remains the same. Numerical tests with simple drag of the form $-\kappa(\rho)\,\dot{\boldsymbol{r}}$ confirmed this, and revealed that main effect is to delay the onset of instability until the ejection from the system becomes possible, *cf.* Fig. 2 (c). Therefore, with a drag, the ejection becomes more likely, while chaotic orbits (Fig. 2 (b)) become rarer. After the test body leaves the mass M, the evolution is identical to the classical restricted planar circular three-body problem.

2.3. Three-body instability

In this section, we drop the assumptions of planar motion and negligible mass of the third body. Without these simplifying assumptions, the full system of nine equations describing the motion of the three masses can also be transformed to the co-rotating system. Very lengthy calculations for full system show that the criteria (8) nearly persist. Using quantifier elimination [30, 31] for stability analysis of the linearized 18-order eigensystem we found that instability is present if

$$\frac{M}{d^3} < \frac{4}{3}\pi\rho < \frac{M + 3m\,(1+\mu/M)^{-1}}{d^3}\,, \tag{18a}$$

$$\frac{4}{3}\pi\rho < \frac{1}{2}\frac{m}{d^3}\frac{M+\mu-m/8}{M+\mu+m}\,(1+\mu/M)^{-1}\,. \tag{18b}$$

The new factor in (18) is the mass of the third body equal to μ. For $\mu \to 0$, (18) reduces to (8). Again, only (18a) is of astrophysical interest. Using orbital frequency

$$\omega^2 = \frac{G(m+\mu+M)}{d^3}\,,$$

and internal frequency

$$\omega_{\mathrm{c}}^2 = \tfrac{4}{3}\,\pi G\,\rho\,,$$

we may rewrite (18a) as

$$\omega^2 + \frac{G(m+\mu)}{d^3} < \omega_{\mathrm{c}}^2 < \omega^2 + \frac{G(m+\mu)}{d^3} + \frac{3Gm}{d^3}\,(1+\mu/M)^{-1}\,.$$

The instability is a consequence of internal and orbital frequency overlap. The width of the resonance is proportional to the "forcing" mass m and reduced by a factor depending on the mass ratio μ/M. The most important is magnitude of mass m, because it increases the orbital frequency allowing for the resonance. Simultaneously, it increases the width of the instability window.

3. Discussion of potential astrophysical sites of the instability

3.1. Massive binaries

The application of the results from Sect. 2.1 to a massive star is not straightforward because the "core" is not well-defined and separated from the envelope. Red supergiants are indeed objects with nearly point-like core and extended low-density envelope. However, the radius separating these two regions is a matter of convention. It is also not clear what really will happen if instability becomes operational. The Thorne–Żytkov objects are an exception because central object is indeed well-approximated by the point mass.

To overcome these difficulties, we adopted the following procedure: a star with total mass M_* and radius R_* is artificially divided into two parts: *(i)* central "core" region with $r < \xi$, and *(ii)* outer envelope with $R_* > r > \xi$. Now, the instability criteria (18) are functions of parameter ξ with

$$\mu = \tilde{m}(\xi)\,, \qquad M = M_* - \tilde{m}(\xi)\,, \qquad \rho = \rho(\xi)\,, \tag{19}$$

where $\tilde{m}(\xi)$ denotes the mass enclosed by the sphere with radius ξ. To further reduce complexity (dimensionality) of the analysis, we assume that the perturbing mass m is as close to the star as possible, *i.e.*, $d = R_*$. The stellar model s15 of [3] with mass $M_* = 12.8\ M_\odot$ and radius $R_* = 3.85$ AU at Si burning stage has been used as an example. The system is stable if

$$\frac{4}{3}\pi\rho(\xi)R_*^3 > (M_* + 3\,m)\left(1 - \frac{\tilde{m}(\xi)}{M_*}\right)\,. \tag{20}$$

In the above example, the instability is present for splitting mass $\tilde{m}$ below $\simeq 4.3\ M_\odot$. Noteworthy, edge of the He core is placed at $\simeq 4.2\ M_\odot$. This result does not significantly vary with perturber mass $1\ M_\odot < m < 100\ M_\odot$. we conclude that splitting the red giant into helium core and hydrogen envelope is the most appropriate. If we treat He core as a point mass, then our model can be applied. It is likely, that during a supernova event in close binary system, the explosion engine will be displaced with respect to geometrical center of the hydrogen envelope. The recently discovered stripped helium core (low-mass white dwarf) in binary system [32] might have been formed in this manner.

3.2. Exoplanets and moons

The models of exoplanet formation and structure often consider a compact core accreting mass in the form of extended low-density envelope [33]. In this situation, dominant is the mass m, *i.e.*, the central star, and the instability occurs if

$$\frac{\rho}{1\,\mathrm{g/cm^3}}\left(\frac{T}{1\,\mathrm{day}}\right)^2 < 0.057\,\frac{M_{\mathrm{env}}}{M_{\mathrm{tot}}}\,, \tag{21}$$

where ρ is the density of the envelope, M_{env} is the mass of accreted envelope and M_{tot} is the total (core+envelope) mass of the protoplanet.

It is not surprising that all of the analyzed exoplanets are stable according to criterion (21). This is also true for so-called Ultra Short Period Planets [34] with orbital period less than a day. However, the stability margin is often small. We may speculate that some of the "puffy planets" [35], *i.e.*, very low density Jupiter-like objects close to the central star, were formed in processes involving ejection of the dense planetary core due to the instability presented in Sect. 2.3. Even if the instability do not lead to the core ejection (because of, *e.g.*, friction), the dissipated energy may inflate the planet. This alone, however, does not explain an absence of the rocky core.

3.3. Globular cluster

Most galactic globular clusters are believed to harbor an intermediate-mass black hole in the center [8, 36, 37]. Therefore, we can use our model to check if central position is stable with respect to perturbations caused by the Galaxy. Using database of Harris (2010 edition) [38] and Eq. (9) we have found that only few out of 157 of GC are unstable, namely Lynga 7, FSR 1735, Terzan 4, 2MS-GC01, 2MS-GC02, BH 261, GLIMPSE02 and GLIMPSE01. In simulations of [10], the instability apparently has not appeared. This is not surprising due to the resonant character of phenomena. It is unlikely to encounter such an instability for a randomly chosen set of

initial conditions. Very interesting is the case of Terzan 3. It is stable if we put $m = 2 \times 10^{11}\ M_\odot$, *i.e.* the mass of the Galaxy without dark matter [39]. However, if we include dark matter, it becomes unstable. Therefore, the search for a central black hole in Terzan 3 might provide a test for the amount of dark matter in the Galaxy. If the dark matter dominates the mass of the Galaxy, then IMBH in Terzan 3 should not exist. This requires further investigation, because orbits of GC are usually not circular, and Galaxy cannot be treated as a point mass. Another complication is caused by infinite radius of popular GC models, like Plummer sphere, see discussion related to (13). More detailed investigation of GC with IMBH and N-body validation of the model from Subsect. 2.3 is in progress.

3.4. LHC black hole

It has been speculated that LHC or other future high-energy experiments might produce artificial black holes that do not evaporate immediately *via* the Hawking radiation [20–22]. Such a black hole would settle at the center of Earth and slowly consume our home planet. We have applied the instability criterion (9) to the Earth–Moon and Earth–Sun systems. Unfortunately, the central position is stable by a wide margin in the sense of instability (8).

4. Conclusions and discussion

The generalized three-body model has been analyzed using analytical and numerical techniques. The instability of the point mass in the core-halo system was found. Analytical criteria (8) and (18) were derived using linearized system, and verified numerically.

Results were applied to astrophysical binaries where one of the companions has a core-halo structure. A few possible sites for the instability were discussed: massive red supergiants in binary system (Subsect. 3.1), formation of the exoplanets (Subsect. 3.2) and globular clusters with intermediate black hole (Subsect. 3.3). The model can also be applied to more exotic situations, *e.g.*, Thorne–Żytkov objects or central black holes of astrophysical and artificial origin.

Binary and multiple systems in astrophysics are rather a rule than an exception, as well as core-halo structure of components, including dark matter halos and central black holes. Therefore, the mechanism of instability presented in this paper may be very common in nature, influencing formation and evolution of the astrophysical bodies and structures on various scales.

Note that our simple analytical model can provide input parameters for more advanced models and numerical simulations. Without such a guide, finding resonant behavior randomly sweeping parameter range is improbable. This is especially important for 3D simulations, which are limited by available computing power to just a few models [40].

In the real world, the instability appears in situations where the perturbing mass m is either very close to the mass M, or is much larger than mass M. In the former case, it is likely that the mass m eventually enters the mass M, with a dynamic drag causing inspiral, sweeping all orbital frequencies. Encountering instability conditions seems inevitable. However, a reduced timescale available to the system may prevent the instability despite its exponential growth. If $m \gg M$, tidal effects are non-negligible and instability asymptotically reduces to the Roche limit. The body with mass M might be destroyed by tidal forces before the resonant instability becomes operational. However, the resonant instability appears before the tidal disruption. The assumption of spherical symmetry and neglected rotation might miss some additional effects, but usually spherical models are good enough to derive instability criteria.

Observational verification of the instability would be difficult in stars and planets, due to the proximity of the Roche limit and complex hydrodynamics with similar timescales. For globular clusters, the model seems more realistic. Minor details such as dynamic drag, non-circular orbits and finite size of the Galaxy are manageable, at least numerically. Unfortunately, the existence of IMBH in the GC center is still under debate. An interesting option is an experimental verification of the instability at space station, using manufactured bodies in the form of, *e.g.*, gas or liquid spheres.

Three-body model needs to be validated. In particular, astrophysical bodies of interest are not rigid (typically gaseous, liquid or composed of particles), and might not react to a driving force as a whole. Ultimately, three-dimensional hydrodynamic model with appropriate treatment of external gravity source, either analytical or numerical, should be used to verify instability in binary stars. For globular clusters, N-body simulations provide a good framework to test the model (work is in progress).

The author would like to thank Piotr Bizoń for reading the manuscript and valuable comments.

REFERENCES

[1] Yue Wang, Shijie Xu, *Aircr. Eng. Aerosp. Technol.* **85**, 8 (2013).
[2] J.-M. Huré, A. Dieckmann, *Astron. Astroph.* **541**, A130 (2012).
[3] S.E. Woosley, A. Heger, T.A. Weaver, *Rev. Mod. Phys.* **74**, 1015 (2002).
[4] N. Haghighipour, *Contemp. Phys.* **52**, 403 (2011).
[5] M.J. Kuchner, *Astrophys. J.* **596**, L105 (2003).
[6] A. Léger *et al.*, *Icarus* **169**, 499 (2004).
[7] S. Umbreit, F.A. Rasio, *Astrophys. J.* **768**, 26 (2013).
[8] M.-Y. Sun *et al.*, *Astrophys. J.* **776**, 118 (2013).

[9] A. Feldmeier *et al.*, *Astron. Astroph.* **554**, A63 (2013).
[10] N. Lützgendorf, H. Baumgardt, J.M.D. Kruijssen, *Astron. Astroph.* **558**, A117 (2013).
[11] N. Lützgendorf *et al.*, *Mem. Soc. Astron. Italiana* **84**, 129 (2013).
[12] N. Lützgendorf *et al.*, *Astron. Astroph.* **552**, A49 (2013).
[13] N. Lützgendorf *et al.*, *Astron. Astroph.* **555**, A26 (2013).
[14] K.S. Thorne, A.N. Żytkow, *Astrophys. J.* **212**, 832 (1977).
[15] R.C. Cannon, *Mon. Not. R. Astron. Soc.* **263**, 817 (1993).
[16] R.C. Cannon, P.P. Eggleton, A.N. Żytkow, P. Podsiadlowski, *Astrophys. J.* **386**, 206 (1992).
[17] A.D. Vanture, D. Zucker, G. Wallerstein, *Astrophys. J.* **514**, 932 (1999).
[18] D.D. Clayton, M.J. Newman, R.J. Talbot, Jr., *Astrophys. J.* **201**, 489 (1975).
[19] S. Hawking, *Mon. Not. R. Astron. Soc.* **152**, 75 (1971).
[20] M. Bleicher, P. Nicolini, *J. Phys. Conf. Ser.* **237**, 012008 (2010).
[21] R. Casadio, S. Fabi, B. Harms, O. Micu, *J. High Energy Phys.* **02**, 79 (2010).
[22] D.M. Gingrich, *Phys. Rev. D* **81**, 057702 (2010).
[23] W.D. Arnett, C. Meakin, *Astrophys. J.* **733**, 78 (2011).
[24] R.A. Mardling, *Lect. Notes Phys.* **760**, 59 (2008).
[25] M.J. Capiński, P. Zgliczyński, *Nonlinearity* **24**, 1395 (2011).
[26] L.D. Landau, E.M. Lifshitz, *Mechanics*, Oxford: Pergamon Press, 1969, 2nd ed.
[27] S. Chandrasekhar, *Astrophys. J.* **138**, 1182 (1963).
[28] P.-G. Gu, D.N.C. Lin, P.H. Bodenheimer, *Astrophys. J.* **588**, 509 (2003).
[29] G. Meylan, D.C. Heggie, *Astron. Astroph.* **8**, 1 (1997).
[30] A. Strzeboński, *Mathematica J.* **7**, 525 (2000).
[31] R. Liska, S. Steinberg, *Computer J.* **36**, 497 (1993).
[32] P.F.L. Maxted *et al.*, *Mon. Not. R. Astron. Soc.* **418**, 1156 (2011).
[33] G. Laughlin, P. Bodenheimer, F.C. Adams, *Astrophys. J. Lett.* **612**, L73 (2004).
[34] K.C. Sahu *et al.*, *Nature* **443**, 534 (2006).
[35] J.D. Hartman *et al.*, *Astrophys. J.* **742**, 59 (2011).
[36] D. Merritt, *Dynamics and Evolution of Galactic Nuclei*, Princeton University Press, 2013.
[37] M. den Brok, G. van de Ven, R. van den Bosch, L. Watkins, *Mon. Not. R. Astron. Soc.* **438**, 487 (2014).
[38] W.E. Harris, *Astron. J.* **112**, 1487 (1996).
[39] S. Sikora, Ł. Bratek, J. Jałocha, M. Kutschera, *Astron. Astroph.* **546**, A126 (2012).
[40] T. Handy, T. Plewa, A. Odrzywołek, *Astrophys. J.* **783**, 125 (2014).